Influence of Tropical Cyclones on Seasonal Ocean Circulation in the South China Sea

Guihua Wang[1], Zheng Ling[1,2], and Chunzai Wang[3]

1. State Key Laboratory of Satellite Ocean Environment Dynamics, Second Institute of Oceanography, SOA, Hangzhou, China

2. CPEO, Ocean University of China, Qingdao, China

3. Physical Oceanography Division, NOAA/Atlantic Oceanographic and Meteorological Laboratory, Miami, Florida, USA

[1] Abstract: The seasonal variability of South China Sea (SCS) ocean circulation influenced by tropical cyclones (TCs) is studied by using satellite QuikSCAT wind data, Sverdrup theory and a reduced-gravity model. TCs can induce a positive (negative) wind stress curl in the northwestern (southeastern) SCS in summer, and a positive wind stress curl for the whole SCS in winter. With these wind stress curls induced by TCs, the cyclonic gyre in the northern SCS and the anticyclonic gyre in the southern SCS are intensified in summer. In winter, the cyclonic gyre in the northern SCS is intensified and the gyre in the southern SCS is weakened except in November and December when the both gyres are enhanced. The model results show that the dipole structure off center Vietnam in summer is intensified and the eddy off northwestern Luzon Island in winter is weakened by TCs. The present paper shows that TCs can affect both large-scale and meso-scale SCS ocean circulation, suggesting that studies including the effect of TCs are necessary to help improve our understanding of SCS ocean circulation dynamics.

Keywords: South China Sea, Ocean circulation, tropical cyclones

1. Introduction

[2] The South China Sea (SCS) is the largest semi-enclosed marginal sea in the tropical western Pacific (Figure 1). Its upper layer circulation is driven mainly by the monsoon, with additional influence from the Kuroshio in its northern part [e.g., *Qu*, 2000; *Su*, 2004]. In winter there is a basin-wide cyclonic gyre, while in summer the circulation splits into a weakened cyclonic gyre north of about 12°N and a strong anticyclonic gyre south of 12°N. These large-scale circulations show a large seasonality, having a relatively short thermocline adjustment time of 1 to 4 months [*Liu et al*., 2001]. Associated with these gyres, there is a dipole structure off central Vietnam in summer [*Wang et al*., 2006] and an alternating eddy in the eastern SCS in winter [*Wang et al*., 2008].

[3] The SCS is among the areas in the northwest Pacific that are often affected by tropical cyclones (TCs). TCs, which affect the SCS, are generated either in the SCS or in the northwest Pacific. As shown in *Gray* [1968], the location and occurrence of the TC formation in the northwest Pacific show a seasonal variability. Seasonal variation of TCs generated over the SCS is largely attributed to the Asian monsoon system, which has been discussed in previous work [*Liang*, 1991, 1998; *Wang et al*., 2007].

[4] Several studies have examined the SCS response to TCs. *Chu et al*. [2001] used the Princeton Ocean Model to investigate the SCS response to TC Ernie and studied the sea surface temperature cooling to the right of TC track and a very strong divergent upper layer current. *Lin et al*. [2003] combined several data sets to show the effects of TCs on chlorophyll and marine life. However, how and why TCs affect SCS

seasonal ocean circulation is not previously documented. The purpose of the present paper is to focus on the effect of TCs on seasonal ocean circulation in the SCS by using observational data, a theoretical model and a numerical model. This includes the influence of TCs on large-scale ocean circulation and meso-scale eddies over the SCS.

2. Data Sets

[5] The main TC dataset covers the period of 2000-2007. The TC dataset is provided by the Japan Meteorological Agency (JMA). The starting year of 2000 is chosen because it is the beginning of a complete year for the QuikScat wind data. The TC dataset includes 6-hourly positions of each TC, its impact radius, as well as its associated minimum center pressure and maximum wind speed. We choose all TCs that can have an impact on the SCS, including TCs in the area of 0-22.5°N and 98.5°E-120.5°E.

[6] The wind dataset used here is from the scatterometer SeaWinds on space mission QuikSCAT of the National Aeronautics and Space Administration (NASA), one of the best-resolved wind products available. The spatial resolution is 0.25° latitude by 0.25° longitude and the temporal resolution is 1 day. The data time period spans from 2000 to 2007. To examine the influence of TCs on ocean circulation over the SCS, we reconstruct two sets of wind forcing: one is the original dataset including all TCs and the other one is to exclude all TCs. We use a simple linear interpolation in time to reconstruct the wind forcing for those periods in which we exclude TCs. The wind stress curls are calculated from the wind datasets with a drag coefficient

depending on wind speed [*Yin et al*., 2007].

[7] To verify the model results, we also use a multiple altimeter sea surface height anomaly dataset on a grid of 1/8° latitude by 1/8° longitude from the U.S. Naval Research Laboratory. The dataset is derived from the TOPEX/POSEIDON (T/P), European Remote Sensing (ERS) and Geosat Follow On (GFO), with the orbit error and tides removed as discussed by *Jacobs et al*. [2002]. This product is a daily dataset covering the period from January 1993 to December 2000. To investigate how TCs affect the sea surface height during that period, the JMA TC dataset from 1993 to 2000 is also used.

3. Methods

[8] We used a theoretical model to estimate the total transport stream function for flow integrated in the entire water column. The Sverdrup theory model [e.g., *Pedlosky*, 1996] is:

$$\psi(x) = -\frac{1}{\rho\beta}\int_{x}^{x_E} curl(\tau)dx\,,$$

where ρ is the density of the seawater and x_E represents the ocean eastern boundary. The boundary condition is $\psi = 0$ at x_E. This simple model has been successfully applied to study the SCS ocean circulation [*Shaw et al*., 1999; *Yang et al*., 2003; *Liu et al*., 2001]. *Liu et al*. [2001] further verified that the total transport and the upper ocean transport are comparable in magnitude and similar in spatial pattern.

[9] A 1.5-layer nonlinear reduced gravity model is also employed to simulate the wind-driven upper ocean circulation including meso-scale eddies. The validity and effectiveness of such a simple model to study the SCS circulation dynamics over deep water have been demonstrated by many studies [e.g., *Metzger and Hurlburt*, 1996; *Liu*

et al., 2001; *Wang et al*., 2006, 2008]. The model equations can be written as:

$$\frac{\partial U}{\partial t}+U\frac{\partial u}{\partial y}+V\frac{\partial u}{\partial y}+u\frac{\partial U}{\partial x}+v\frac{\partial U}{\partial y}-fV=-g'h\frac{\partial h}{\partial x}+A_h(\frac{\partial^2 U}{\partial x^2}+\frac{\partial^2 U}{\partial y^2})-\nu\frac{\partial u}{\partial z}\Big|_h+\nu\frac{\partial u}{\partial z}\Big|_{z=0} \quad (1)$$

$$\frac{\partial V}{\partial t}+U\frac{\partial v}{\partial x}+V\frac{\partial v}{\partial y}+u\frac{\partial V}{\partial x}+v\frac{\partial V}{\partial y}+fU=-g'h\frac{\partial h}{\partial y}+A_h(\frac{\partial^2 V}{\partial x^2}+\frac{\partial^2 V}{\partial y^2})-\nu\frac{\partial v}{\partial z}\Big|_h+\nu\frac{\partial v}{\partial z}\Big|_{z=0} \quad (2)$$

$$\frac{\partial h}{\partial t}+\frac{\partial U}{\partial x}+\frac{\partial V}{\partial y}=0 \quad (3)$$

where x, y and z are the conventional Cartesian coordinates; u and v are the components of velocity corresponding to x and y, respectively; U and V are the total flows integrated over the entire water column from the thermocline to the surface; h is the thermocline depth; ρ is the density; $g' = g\triangle\rho/\rho_0$ is the reduced gravity; ν is the vertical diffusion coefficient and A_h is the lateral friction coefficient.

[10] The model land-sea boundary is along the 200 m isobath (Figure 1). The 200 m isobath is chosen because it is the bottom of the SCS thermocline and the 1.5 layer reduced-gravity model cannot be applied to the region shallower than the thermocline or the outcrop region to the thermocline. We open the Luzon Strait to include the Kuroshio as a driving force and specify a Kuroshio-related input along the zonal section 122°E-124.5°E (18°N). The Kuroshio output along the zonal section 123^oE-126^oE (24.5°N) as an open boundary condition is self-determined, by momentum equation, as done by *Hurlburt and Thompson* [1980]. The reduced gravity is set to $g'=0.03$ m s^{-2}. The lateral friction coefficient is 500 m^2s^{-1} and the initial thermocline depth is 200 m. The model resolution is on a grid of 0.25° latitude by 0.25° longitude. The grid size is smaller than the first baroclinic Rossby radius of deformation for the deep basin of the SCS, which is larger than 50 km [*Gan and Cai*,

2000]. The model is spun up with the winds switched on gradually from the rest to the wind distribution of January 1, 2000 over a 1-month period. The model is then run with the wind forcing data of the whole year from January 1 to December 31, 2000. The model run is repeated for four years until the ocean circulation reaches a quasi-equilibrium state. Then, the model is forced from January 1, 2000 to December 31, 2007 by the two wind forcing datasets mentioned in section 2.

4. Results

4.1 Tropical cyclones and wind stress curls

[11] Tropical cyclones (TCs), which can affect the SCS, are generated either in the SCS and northwest Pacific. Figure 2 shows the 12-hour positions of all TCs over the SCS. During January and February, there are no TCs in the SCS. TCs generated in the northwest Pacific appear over the SCS from March to December. They were located mostly in the northeastern SCS from July to August, in north of 12°N from September to October, and in the middle SCS from November to December. August and November are two active months of TCs generated in the northwest Pacific (also see Table 1), indicating a bimodal distribution in the number of TCs generated in the northwest Pacific that reach to the SCS. TCs generated in the SCS occur from May to December. The peak months of SCS-generated TCs are from July to September. SCS-generated TCs are mostly confined north of 12°N except in December when some SCS-generated TCs are in north of the equator (Fig. 2). In particular, SCS-generated TCs are over the northwestern SCS in August and September. An

investigation of physical reasons for cyclogenesis over the SCS is beyond the scope of the present paper.

[12] As demonstrated in previous studies [e.g., *Qu*, 2000; *Wang et al*., 2006; *C. Wang et al*., 2006], the summer mean wind stress curl is positive (negative) in the northwestern (southeastern) SCS, and the winter mean wind stress curl is positive (negative) in the southeastern (northwestern) SCS. The wind stress curl was calculated with the wind forcing without TCs, as shown in Figure 3. Because of the strong northeasterly monsoon flow from October to March, there is a positive wind stress curl in the southwestern SCS and negative wind stress curl in the northeastern SCS. The area of negative part gradually increases during these months. There is also a series of meso-scale wind-stress curl cells with alternating signs along the eastern boundary of the SCS because of island orographic effects [*Wang et al*., 2008]. The southeastern Asian monsoon transition from the winter northeasterly to the summer southwesterly occurs in spring around May. The summer southwesterly monsoon is further developed from June to August, and retreated in September. The wind stress curls in summer reflect the southwesterly flow of the summer monsoon (Figure 3).

[13] Figure 4 shows the monthly mean wind stress curl difference between the original wind forcing and the wind forcing without TCs, i.e., the wind stress curl induced by TCs over the SCS. Generally, from June to October TCs produce the positive (negative) wind stress curl in the northwestern (southeastern) SCS. During November and December a positive wind stress curl is induced over the whole SCS. However, from March to May TC-induced wind stress curl is weak. During January

and February, the wind stress curl difference is zero because there are no TCs over the SCS in these two months (Fig. 4).

4.2 Sverdrup currents

[14] Many previous studies have discussed general ocean circulation in the SCS [e.g., *Qu*, 2000; *Su*, 2004]. Here we use the wind forcing without TCs to calculate the Sverdrup stream function (Fig. 5), as stated in Section 3. From October to March, the winter northeasterly Asian monsoon forces a grand basin-wide cyclonic Sverdrup flow, which contains two sub-gyres: the northern SCS gyre and the southern SCS gyre. These two cyclonic gyres are divided by a leptosomatic anticyclonic gyre around 14°N (Figure 5). However, the narrow anticyclonic gyre here may be illusive. First, all previous observations including hydrographic data and drifter data didn't show this circulation gyre [e.g., *Qu*, 2000; *Centurioni*, 2004]. Second, the Sverdrup relation can only be applied to the phenomenon in which spatial scale is larger than the baroclinic deformation radius (around 100 km in the SCS); however, the anticyclonic gyre is obtained by a strong narrow (around 50 km) negative wind stress curl near Manila Bay as shown in Figure 3. During boreal spring of the Asian monsoon transition period from the winter to summer monsoon, SCS ocean circulation also begins to change. From May the double gyres with a cyclonic gyre north of about 12°N and an anticyclonic gyre south start to develop. The double gyres are further developed in June and July, and matured in August.

[15] How do TCs affect SCS ocean circulation? Figure 6 shows the Sverdrup

stream function difference between the original wind forcing and the wind forcing without TCs. The cyclonic Sverdrup flow with the two sub-gyres from November to December is enhanced by the more positive wind stress curls (Fig. 4). In particular, the enhancement of the two sub-gyres is the largest in November because many TCs are reached to the SCS from the northwest Pacific in November (Fig. 2). However, the southern sub-gyre is weakened and the northern one is enhanced in October because TCs produce negative and positive wind stress curls in the southeastern and northwestern SCS, respectively (Fig. 4). The cyclonic Sverdrup flow in the months of January to March is not affected by TCs since there are no (or few) TCs over the SCS during these months.

[16] From June to September, the cyclonic gyre and anticyclonic gyre are generally enhanced (Fig. 6) by the TC-induced positive and negative wind stress curls in the northwestern and southeastern SCS, respectively (Fig. 4). It should be pointed out that the two gyres are much enhanced from July to September because these three months are the time with more TCs in the northern SCS. Although the northern cyclonic sub-gyre is still enhanced in May, the southern anticyclonic sub-gyre is weakened because the TC-induced positive wind stress curl covers over the whole SCS in this month.

[17] If we suppose that the upper ocean layer transport is conserved, we can estimate the transport of the western boundary current as listed in Table 2 from the Sverdup flow of Figure 6. It is shown that the western boundary current also has a seasonal variation. The western boundary current is the strongest in December and the

weakest in April. The contribution of TCs to the western boundary transport over the SCS can range from 0.03 Sv to 0.88 Sv.

4.3 Model Results

[18] The above observations show that TCs can affect the strength of SCS large-scale ocean circulation. However, Sverdrup theory is only the first estimate of ocean circulation and it may be over-simple for ocean circulation over the SCS. Sverdrup theory provides an estimate of ocean transport changes with an assumption that the ocean is in near-equilibrium with surface wind forcing. This assumption neglects the details of baroclinic wave processes in adjusting the ocean response to wind forcing changes [*Liu et al.*, 2001]. However, the effect of TCs (with a lifetime of several days) on SCS ocean circulation may last for 1-4 months due to ocean adjustment. This accumulative effect on the SCS circulation driven by TCs has been neglected by Sverdrup theory. At the same time, there are many meso-scale eddies embedded in the SCS large-scale circulation. It is also unknown about the effect of TCs on the strength of meso-scale eddies over the SCS. Thus, we carry out a series of numerical model experiments to investigate how TCs affect the seasonal SCS ocean circulation including large-scale circulation and meso-scale eddies. These experiments use two sets of wind data discussed in Section 2 to force the reduced gravity model.

[19] Figure 7 shows the modeled monthly mean thermocline depth over the SCS from 2000 to 2007 with the reduced-gravity model, which is driven by the wind field without TC-generated wind. The winter basin-wide cyclonic Sverdrup flow is built up well from October. The anticyclonic and cyclonic alternating eddies are also produced

from December to April in the model. The summer large-scale circulation pattern is a cyclonic gyre north of 12°N and an anticyclonic gyre south of 12°N. The summer meso-scale circulation is characterized with a dipole eddy structure off centre Vietnam: northern one is a cyclonic eddy and southern one is an anticyclonic eddy. All of these are consistent with previous studies [*Metzger and Hurlbut*, 1996; *Liu et al.*, 2001; *Wang et al*., 2006, 2008]. This indicates that the model can capture the wind-driven both large-scale circulation and eddies' dynamics over the SCS.

[20] The modeled monthly mean thermocline depth difference between the original wind forcing and the wind forcing without TCs is displayed in Figure 8. Generally, the northwestern part of basin-wide cyclonic flow is enhanced and the southeastern part is weakened from October to March except in November and December when the whole winter cyclonic gyre is intensified as TCs are located in the middle SCS in these two months (Fig. 2). Figure 8 also shows that the cyclonic eddy northwest of Luzon Island is weakened in winter (the difference is positive). The weakened eddy results from a negative wind stress curl which is produced as TCs pass Luzon Island (i.e., the effect of Luzon Island). It is interesting to note that TCs still can influence SCS thermocline depth in January to March (Fig. 8) although there are few TCs in these three months (Fig. 2). This may reflect the accumulative effect of TCs on the SCS mentioned early. In summer, both the cyclonic circulation in the northern SCS and the anticyclonic gyre in the southern SCS are generally intensified (Figure 8). Associated with these strengthened gyres, a strong dipole off centre Vietnam is also found from July to September as showed in Figure 8. The dynamic

processes of how TCs affect the dipole can be described as follows. The strengthened cyclonic (anticyclonic) gyre amplifies a stronger southward (northward) boundary current along the northwestern (southwestern) SCS western boundary, which further transports more positive (negative) vorticity to the centre Vietnam through the inertial process, thus the dipole is strengthened [*Wang et al*., 2006].

[21]Availability of the daily sea surface height data from 1993 to 2000 provides us an opportunity to examine whether observations support or are consistent with the model findings of the effect of TCs on the SCS. Figures 9a and 9b show the observed sea surface height difference with and without TCs influences, and the TC distribution during summer (June to August), respectively. The model-simulated effect of TCs on the thermocline depth and its corresponding TC distribution during summer are shown in Figs. 9c and 9d. Note that the period of observations (from 1993 to 2000) is different from that of modeling simulation (from 2000 to 2007). However, this is not a problem since we are interested in the general pattern effect of TCs on the SCS rather than a detailed comparison. We choose the summer mean because TCs are frequent during summer and the positions of TCs are mostly located in northern SCS in both of these two periods (Figure 9b and Figure 9d). Figure 9a shows the cyclonic gyre in the northern SCS and the anticyclonic gyre in southern SCS are enhanced by TCs. Associated with these two enhanced gyres, a dipole off central Vietnam is also strengthened by TCs. The observed results are generally consistent with the summer pattern from the model simulation (Figure 9c), although there are some differences in detail.

5. Summary and Discussions

[22] Based on the observations and model results, we find that a positive (negative) wind stress curl in the northwestern (southeastern) SCS is produced by TCs in summer, and a positive wind stress curl is generally induced over the whole SCS in winter. With these TC-induced wind stress curls, the northern (southern) part of the winter cyclonic gyre is intensified (weakened) except in October and November when both the gyres are strengthened. The summer TC-induced wind stress curls enhance the cyclonic gyre in the northern SCS and the anticyclonic gyre in southern SCS.

[23] The numerical model results further reveal the meso-scale eddies in the SCS also can be affected by TCs. The cyclonic eddy northwest of Luzon Island is slacked because of a negative wind stress curl anomaly produced by TCs in winter. The dipole structure off central Vietnam is enhanced because the basin-wide gyre is strengthened by TC-induced wind forcing.

[24] Although few TCs are over the SCS from January to March, the model results show that during these months the SCS thermocline depth is still affected by TCs. This provides an evidence of the accumulative effect of TCs on the SCS ocean circulation.

[25] In order to exclude the influence of TCs, we use a simple linear interpolation in time to reconstruct wind data for the period with TCs appeared over the SCS. However, TCs can cause the ocean cooling as discussed in Section 1 [*Chu et al*., 2001; *Lin et al*., 2003], so the resulting SST changes can in turn modify the wind field in several ways [*Gill*, 1980; *Lindzen and Nigam*, 1987] over the SCS even after TCs

have disappeared from the SCS. Such air-sea interactions including the heat fluxes and salt fluxes have been neglected in this study since the focus of this paper is on SCS response to TCs through momentum fluxes. A further study including the air-sea interaction processes should be helpful to understand the complete pictures of how TCs affect the SCS.

[26] The model simulations show that TCs can affect both the large-scale ocean circulation and meso-scale eddies over the SCS. This suggests that studies considering TC's effect are necessary and helpful to understand the SCS ocean circulation dynamics. Furthermore, a high-resolution three-dimensional model will help us improve the understanding of more complete dynamics such as mixing and the three-dimensional structures' influences of the Kuroshio on the SCS [*Qu et al*., 2008]. Hopefully, the present paper can stimulate more studies of the influence of TCs on the SCS in the near future.

Acknowledgements:

The study was supported by the National Basic Research Program (2007CB816003) and the National Natural Science Foundation of China (Grant #: 40676007,40730843 and 40876004). We thank two anonymous reviewers for their comments and suggestions on this paper.

References

Centurioni, L.R., P. P. Niiler and D. K. Lee ,2004: Observations of Inflow of Philippine Sea Surface Water into the South China Sea through the Luzon Strait. Journal of physical

oceanography,34, 113-121.

Chu P.C, S.H. lu and W.T. Liu,1999: Uncertainty of the South China sea prediction using NSCAT and NCEP winds during tropical storm Ernie 1996,Journal of Geophysical research, 104,11273-11289

Gan, Z.J. and S.Q.Cai, 2001: Geographical and seasonal variability of Rossby Radii in South China Sea, Journal of Tropical oceanography. 20(1), 1-9.

Gill, A. E., 1980: Some simple solutions for heat-induced tropical circulation. Quarterly Journal of the Royal Meteorological Society, 106 447-462.

Gray, W.M., 1968: A global view of the origin of tropical disturbances and storms. Monthly Weather Review, 96, 669-700.

Hurlburt, H.E. and J.D. Thompson, 1980: Numerical study of loop current intrusions and eddy shedding. *Journal of physical oceanography.,* 10, 1611-1651.

Jacobs, G. A., C. N. Barron, D. N. Fox, K. R. Whitmer, S. Klingenberger,D. May, and J. P. Blaha, Operational Altimeter Sea Level Products. Oceanography, 15(1), 13– 21, 2002.

Liang, B. Q., 1991: *The Tropical Atmospheric Circulation System over the South China Sea*, (in Chinese), China Meteorology Press, Beijing.

Liang, B. Q., T. M. Wang, and X. M. Zhou, 1998: The statistical analysis of the tropical cyclone in the Nansha Islands waters, (in Chinese), in *The Studies on the Interaction of the Air-Sea and the Property of Synoptic Climatology in the Nansha Islands Waters,* pp.163-172, edited by Q. R. Zhang and B. Q. Liang, Science Press, Beijing.

Lin, I.-I., W. T. Liu, C.-C. Wu, J. C. H. Chiang, and C.-H. Sui, 2003: Satellite observations of modulation of surface winds by typhoon-induced upper ocean cooling. *Geophysical Research*

Letter 30, 1131.

Lindzen, R.S., and S. Nigam, 1987: On the role of sea surface temperature gradients in forcing low-level winds and convergence in the tropics. *Journal of Atmosphere. Science,* **44**, 2418-2436.

Liu, Z.Y., H.J. Yang and Q.Y. Liu, 2001: Regional dynamics of seasonal variability in the South China Sea. *Journal of physical oceanography*, 31, 272-284.

Metzger E J,Hurlburt H E,1996.Coupled dynamics of the South China Sea, the Sulu Sea, and the Pacific Ocean. Jouranl of Geophysical Research, 101(C5):12331-12352

Qu, T.D., 2000: Upper-Layer circulation in the South China Sea. *Journal of physical oceanography*, 30, 1450-1460.

Qu, T., T. Song, and T. Yamagata, 2009: An introduction to the South China Sea throughflow: Its dynamics, variability, and implication for climate. Dynamics of Atmospheres and Oceans, 47, 3-14

Shaw, P.T., S.Y. Chao and L.L. Fu, 1999: Sea surface height variation in the South China Sea from satellite altimetry. *Oceanologica ACTA*, 22, 1-17.

Su J., 2004: Overview of the South China Sea circulation and its influence on the coastal physical oceanography near the Pearl River Estuary. *Continental Shelf Research*, 24, 1745-1760.

Wang, C., W. Wang, D. Wang, and Q. Wang, 2006: Interannual variability of the South China Sea associated with El Niño. *Journal of Geophysical Research.*, **111**, C03023, doi:10.1029/ 2005JC003333.

Wang G., Chen D. and J.Su, 2008: Winter Eddy Genesis in the Eastern South China Sea due to Orographic Wind-Jets. Journal of Physical Oceanography, .38, 726-732.

Wang G., Su J., Ding Y. and D.Chen, 2007: Tropical Cyclones Genesis over the South China Sea. Journal of Marine Systems. 68(3-4), 318-326.

Wang, G., Chen D. and J. Su, 2006: Generation and Life Cycle of the Dipole in South China Sea Summer Circulation. Jouranl of Geophysical Research, 111, C06002, doi: 10.1029/ 2005JC003314.

Yang H. and Q. Liu (2003), Forced Rossby wave in the northern South China Sea, Deep Sea Research I 50, 917-926.

Yin, X., Z. Wang, Y. Liu, and Y. Xu (2007), Ocean response to Typhoon Ketsana traveling over the northwest Pacific and a numerical model approach, Geophysical Research Letter,34,L21606, doi:10.1029/2007GL031477.

Table 1: Days of tropical cyclones in the South China Sea (SCS) from 2000 to 2007. The bracket in the row of northwest Pacific represents the number of tropical cyclones whose eye center is in the interior of SCS.

Month	1	2	3	4	5	6	7	8	9	10	11	12
Northwest Pacific	0	0	2(2)	1	7(5)	15.5(10)	28(15)	34(20)	30.5(19.5)	19(11.5)	54(48)	18(15.5)
South China Sea	0	0	0	0	9	12	18	24	25	3.5	1.5	2
Total	0	0	2	1	16	27.5	46	58	55.5	22.5	55.5	20

Table 2: Transport (Sv) of the SCS Western Boundary Currents. North is for cyclonic gyre and South is for anticyclonic gyre in summer. North and South are for the north and south sub-cyclonic gyre in winter.

Month		1	2	3	4	5	6	7	8	9	10	11	12
No TCs	North	6.73	6.13	3.99	1.65	1.76	2.38	4.58	5.66	4.62	8.94	9.74	11.50
	South	6.67	5.16	2.92	1.54	1.63	2.67	4.99	5.87	3.57	6.44	6.49	9.16
All TCs	North	6.73	6.13	4.02	1.65	2.15	2.66	4.97	5.97	4.96	9.27	10.33	11.84
	South	6.67	5.16	2.92	1.54	1.63	2.82	5.41	6.29	3.57	5.76	7.37	9.23
TCs Contribution	North	0	0	0.03	0	0.39	0.28	0.39	0.31	0.34	0.33	0.59	0.34
	South	0	0	0	0	0	0.15	0.42	0.42	0	-0.68	0.88	0.07

Figure Captions

Figure 1: Map of the South China Sea. The two isobaths are for 200 m and 2000 m, respectively. The open ocean boundaries are set at 18^{o}N and 24.5^{o}N lines, and the boundary along 126^{o}E is set to a wall.

Figure 2: 12-hour's positions of tropical cyclones (TCs) over the South China Sea (SCS). TCs generated from the northwest Pacific are represented by solid triangle, whereas TCs generated in the SCS is denoted by solid circle.

Figure 3: The wind stress curl (10^{-8} N/m^{3}) calculated from the wind forcing without tropical cyclones. The positive wind stress curl is shaded.

Figure 4: The wind stress curl difference (10^{-8} N/m^{3}) between the original wind forcing and the wind forcing without tropical cyclones. The positive wind stress curl is shaded.

Figure 5: Monthly mean stream function (Sv) forced by the wind without tropical cyclones. The positive stream function is shaded.

Figure 6: Monthly mean stream function difference (Sv) between the original wind forcing and the wind forcing without tropical cyclones. The positive stream function is shaded.

Figure 7: Monthly thermocline depth (m) forced by the wind field without tropical cyclones. Dashed line is for the thermocline depth smaller than 184 m and solid line is for larger than 184 m.

Figure 8: Monthly thermocline depth difference (m) between the original wind forcing and the wind forcing without tropical cyclones. Dashed (solid) line is for negative (positive) thermocline depth difference.

Figure 9: (a) Sea surface height anomaly difference (mm) between the original sea surface height anomaly and the one excluding the periods of tropical cyclones in summer from 1993 to 2000; (b) 12-hour position of tropical cyclones over the South China Sea in summer from 1993 to 2000; (c)

the model simulated thermocline depth difference (m) between the original wind forcing and the wind forcing without tropical cyclones; (d) 12-hour position of tropical cyclones over the South China Sea in summer from 2000 to 2007. In (a) and (c), the positive values are shaded. In (b) and (d) TCs generated from the northwest Pacific are represented by solid triangle, whereas TCs generated in the SCS is denoted by solid circle.

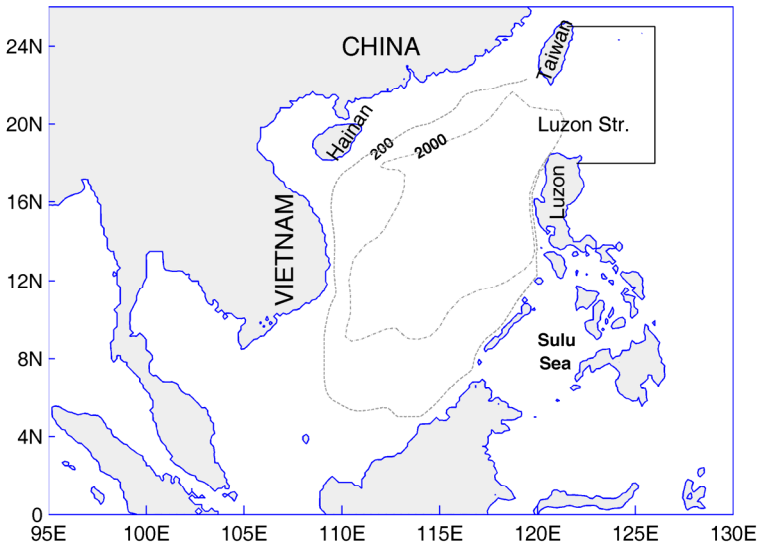

Figure 1: Map of the South China Sea. The two isobaths are for 200 m and 2000 m, respectively. The open ocean boundaries are set at 18^{o}N and 24.5^{o}N lines, and the boundary along 126^{o}E is set to a wall.

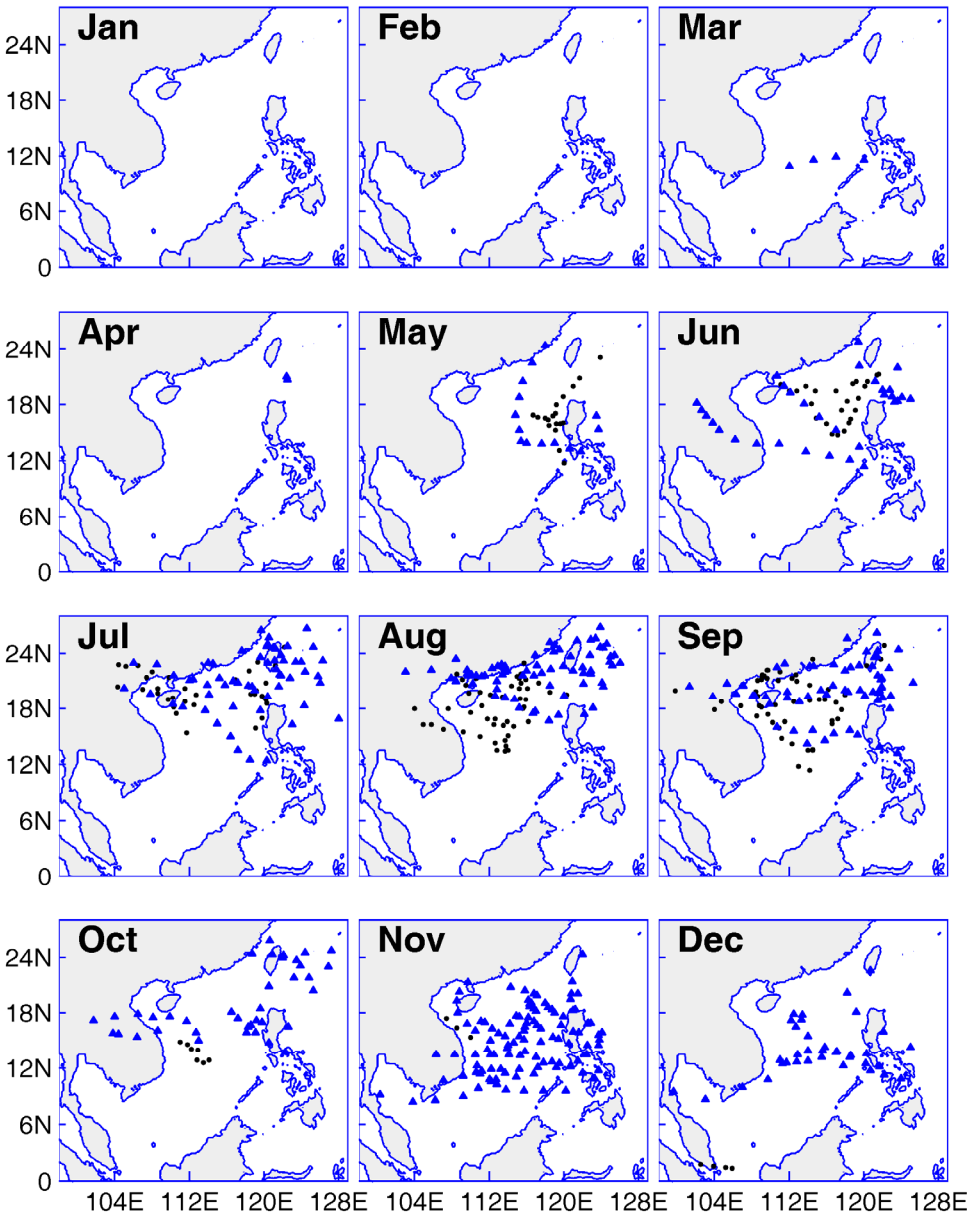

Figure 2: 12-hour's positions of tropical cyclones (TCs) over the South China Sea (SCS). TCs generated from the northwest Pacific are represented by solid triangle, whereas TCs generated in the SCS is denoted by solid circle.

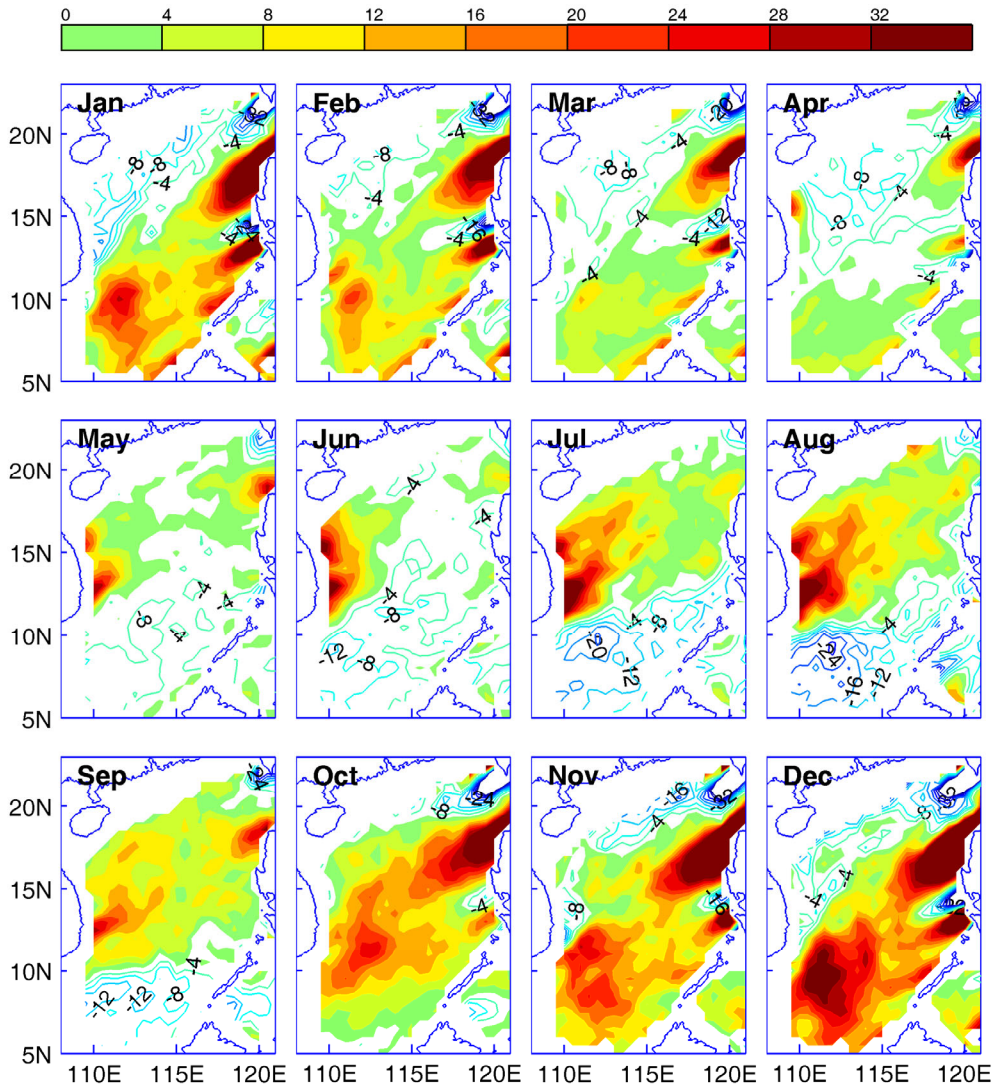

Figure 3: The wind stress curl (10^{-8} N/m^3) calculated from the wind forcing without tropical cyclones. The positive wind stress curl is shaded.

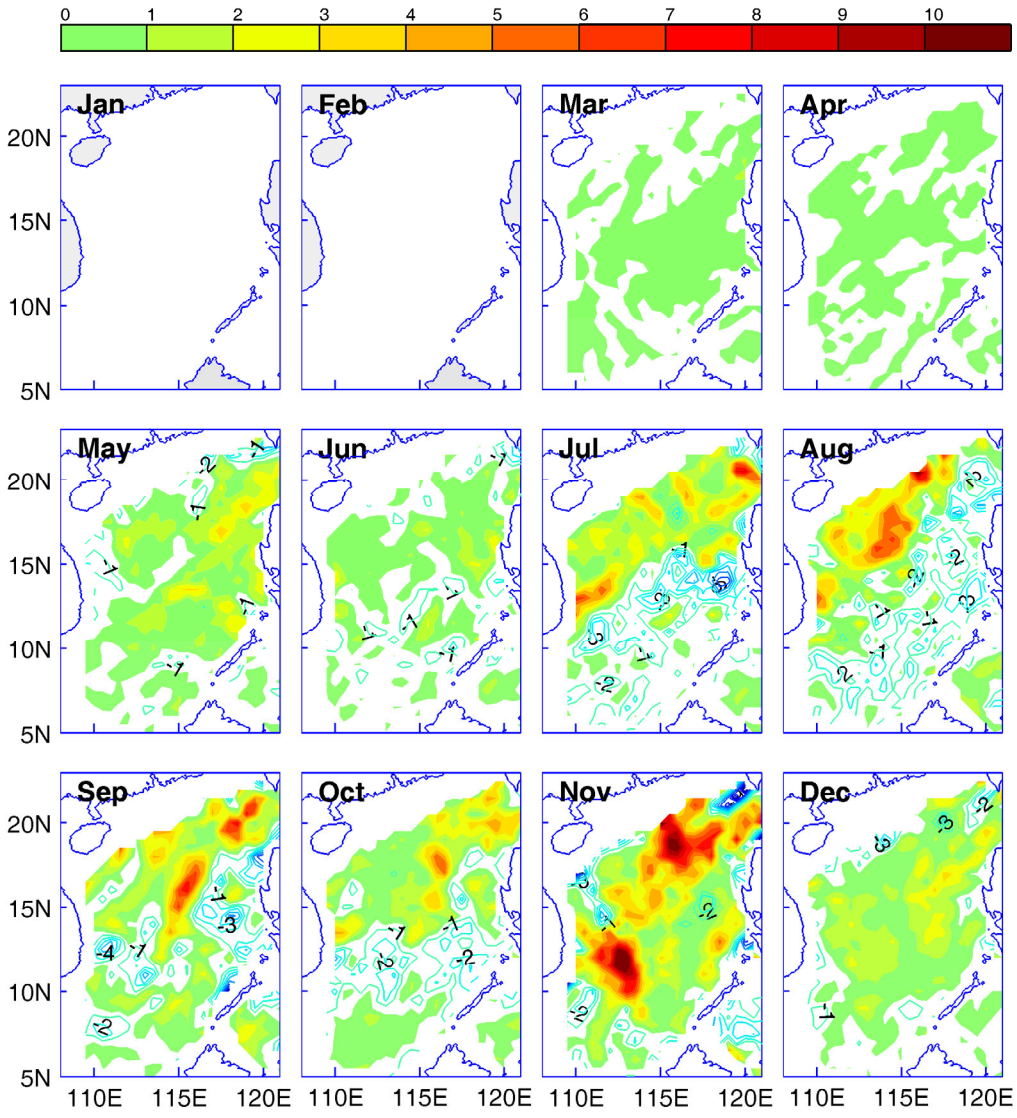

Figure 4: The wind stress curl difference (10^{-8} N/m^3) between the original wind forcing and the wind forcing without tropical cyclones. The positive wind stress curl is shaded.

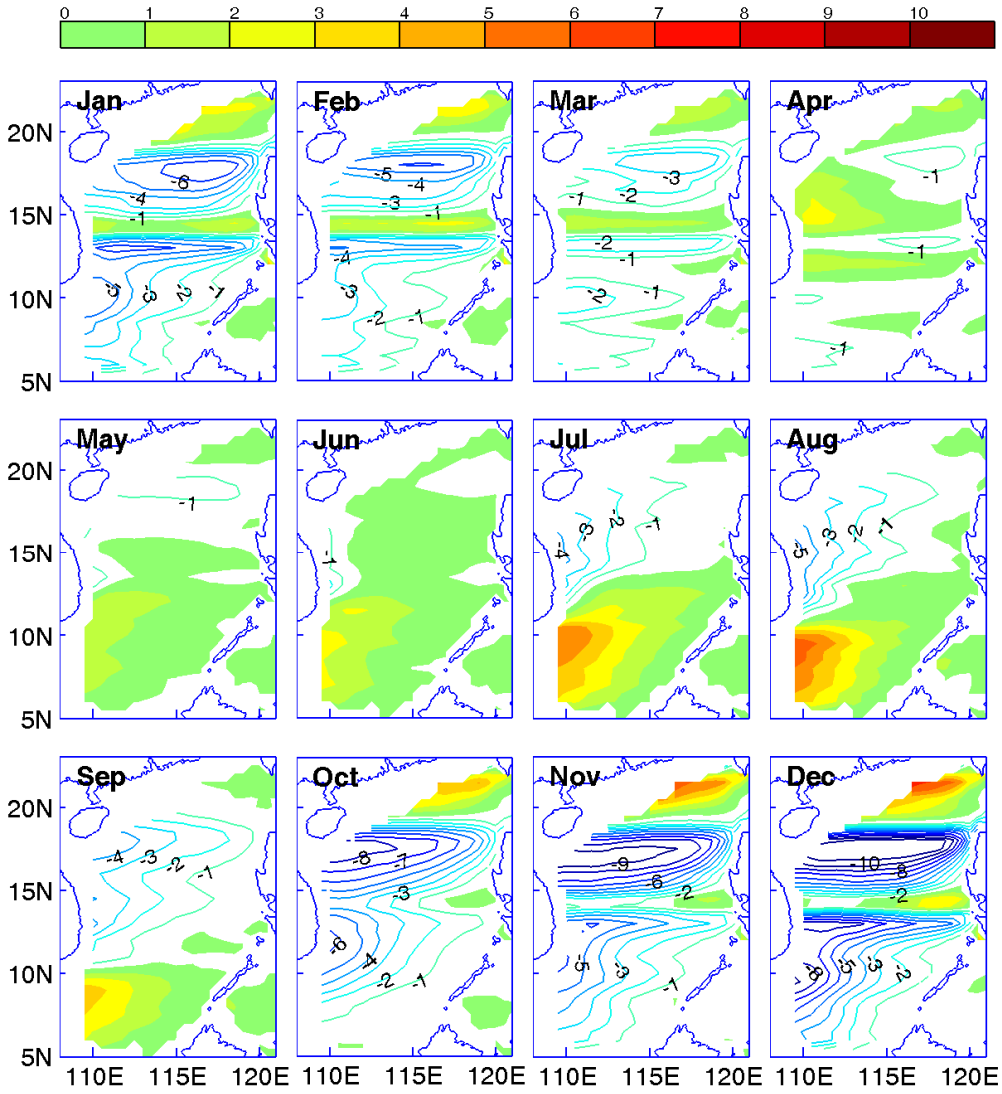

Figure 5: Monthly mean stream function (Sv) forced by the wind without tropical cyclones. The positive stream function is shaded.

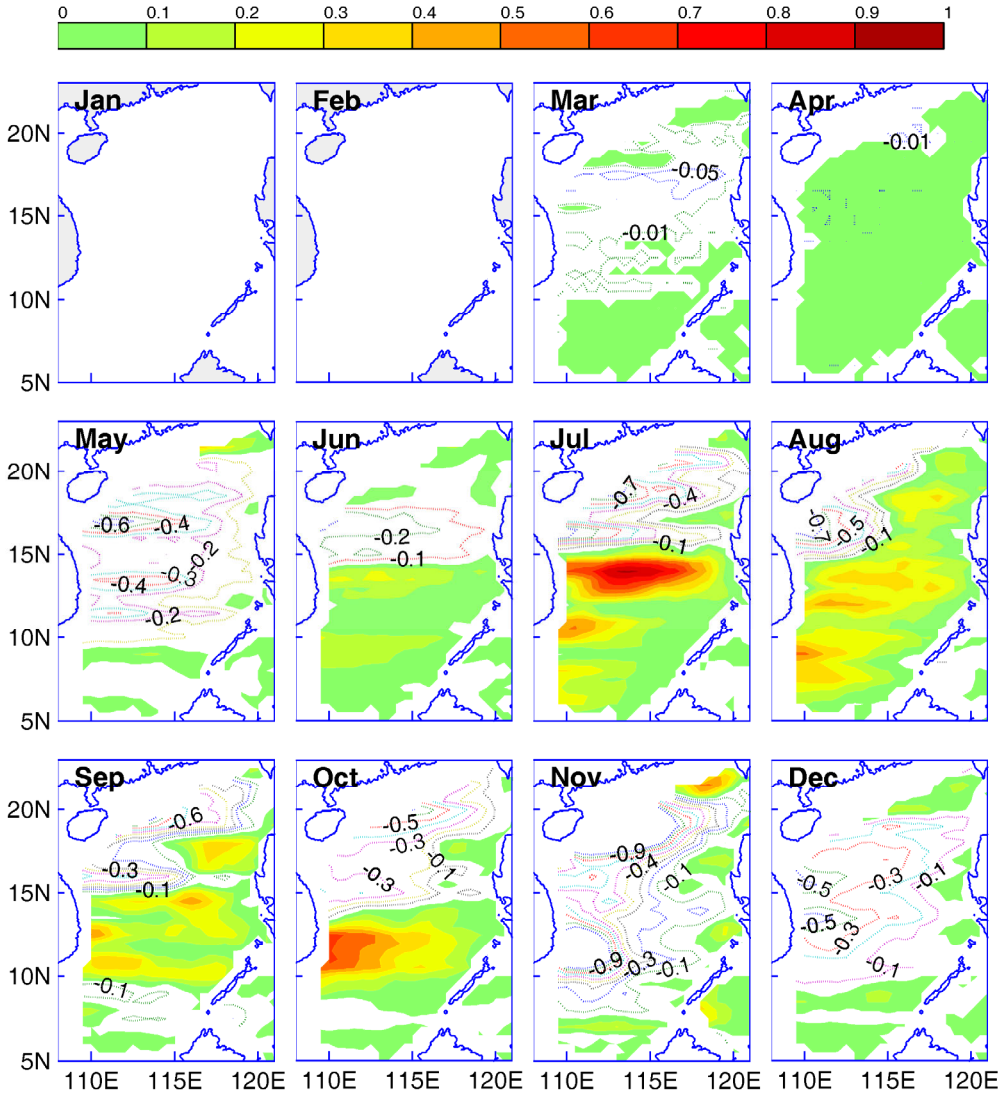

Figure 6: Monthly mean stream function difference (Sv) between the original wind forcing and the wind forcing without tropical cyclones. The positive stream function is shaded.

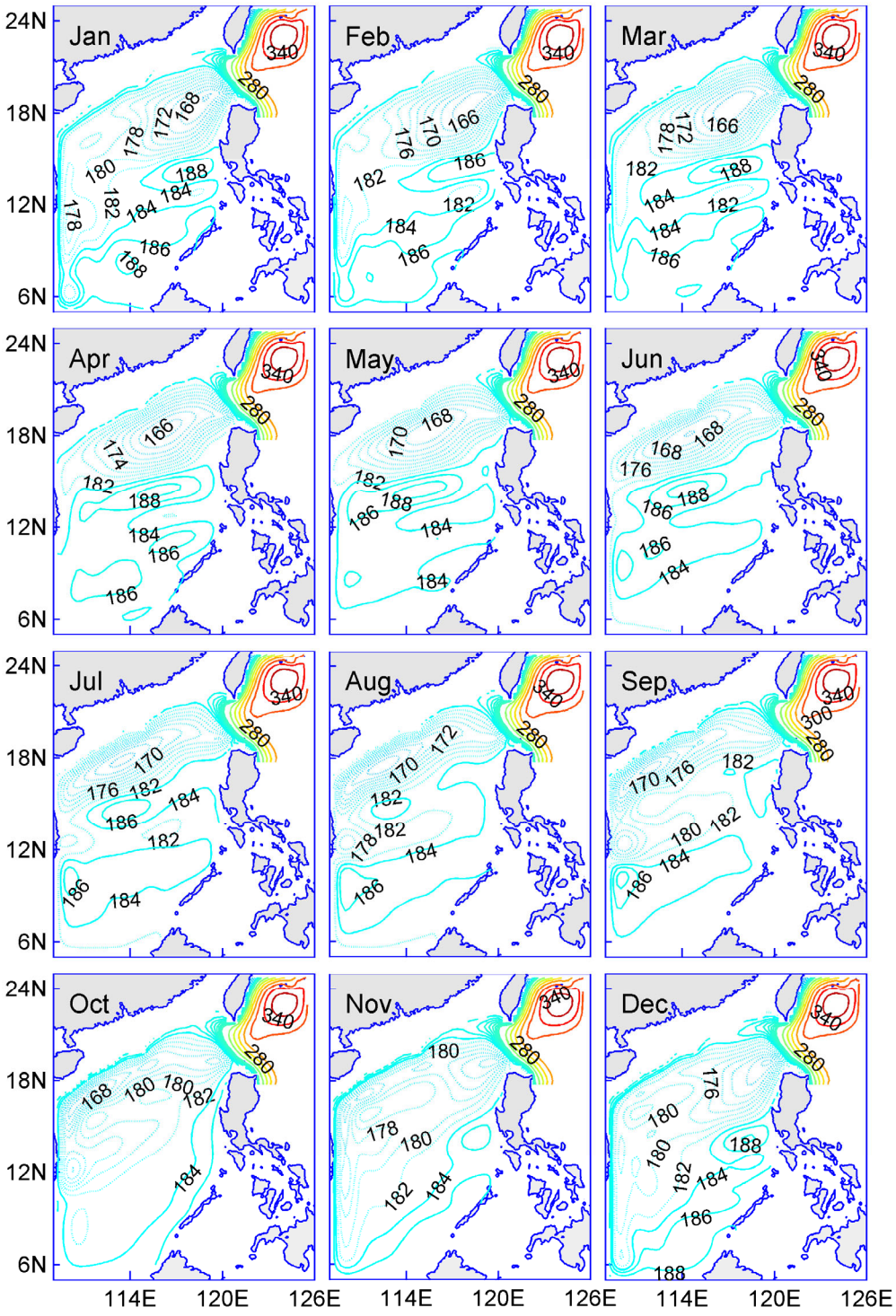

Figure 7: Monthly thermocline depth (m) forced by the wind field without tropical cyclones. Dashed line is for the thermocline depth smaller than 184 m and solid line is for larger than 184 m.

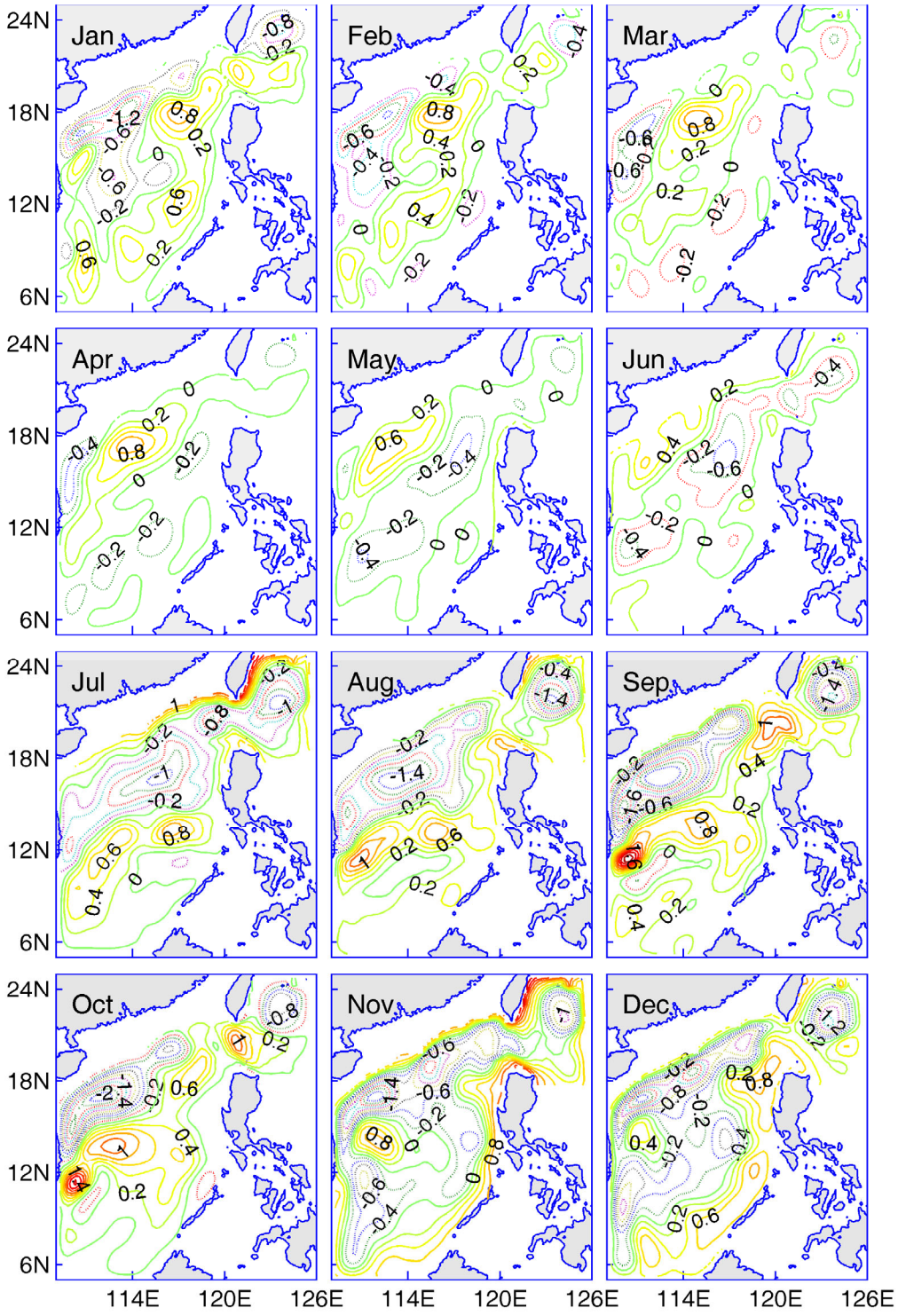

Figure 8: Monthly thermocline depth difference (m) between the original wind forcing and the wind forcing without tropical cyclones. Dashed (solid) line is for negative (positive) thermocline depth difference.

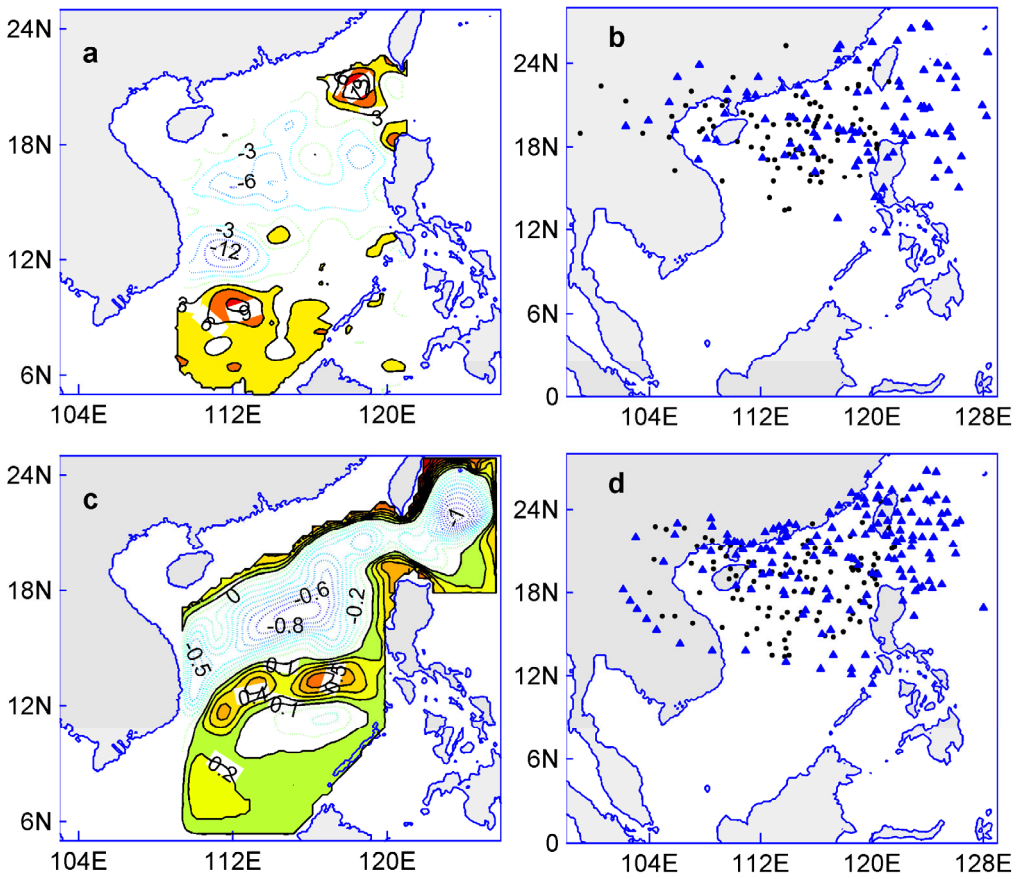

Figure 9: (a) Sea surface height anomaly difference (mm) between the original sea surface height anomaly and the one excluding the periods of tropical cyclones in summer from 1993 to 2000; (b) 12-hour position of tropical cyclones over the South China Sea in summer from 1993 to 2000; (c) the model simulated thermocline depth difference (m) between the original wind forcing and the wind forcing without tropical cyclones; (d) 12-hour position of tropical cyclones over the South China Sea in summer from 2000 to 2007. In (a) and (c), the positive values are shaded. In (b) and (d) TCs generated from the northwest Pacific are represented by solid triangle, whereas TCs generated in the SCS is denoted by solid circle.